Multiple-scale neuroendocrine signals connect brain and pituitary hormone rhythms

Classification: Biological Sciences: Neuroscience

Multiple-scale neuroendocrine signals connect brain and pituitary hormone rhythms

Authors: Nicola Romanò[1*#], Anne Guillou[1], David J. Hodson[2,3], Agnès O Martin[1], Patrice Mollard[1*]

Affiliations: [1]IGF, CNRS, INSERM, Univ. Montpellier, F-34094 Montpellier, France; [2]Institute of Metabolism and Systems Research (IMSR) and Centre of Membrane Proteins and Receptors (COMPARE), University of Birmingham, Edgbaston, B15 2TT, UK. [3]Centre for Endocrinology, Diabetes and Metabolism, Birmingham Health Partners, Birmingham, B15 2TH, UK.

*Correspondence to:
Nicola Romanò, University of Edinburgh, Centre for Integrative Physiology, Edinburgh, EH8 9XD, UK,
Tel.: +44 131 650 3874, email: nicola.romano@ed.ac.uk or
Patrice Mollard, Institut de Génomique Fonctionnelle, 141 rue de la Cardonille, F-34094 Montpellier, France, tel. : +33 4334359270, email : patrice.mollard@igf.cnrs.fr

#Current address: University of Edinburgh, Centre for Integrative Physiology, Edinburgh, EH8 9XD, UK

Running title: A neurohemal code for hormone secretion

Key words: dopamine, prolactin, rhythms, hypothalamus

ABSTRACT

Small assemblies of hypothalamic 'parvocellular' neurons release their neuroendocrine signals at the median eminence to control long-lasting pituitary hormone rhythms essential for homeostasis. How such rapid hypothalamic neurotransmission leads to slowly-evolving hormonal signals remains unknown. Here, we show that the temporal organization of dopamine release events in freely-behaving animals relies on a set of characteristic features that are adapted to the dynamic dopaminergic control of pituitary prolactin secretion, a key reproductive hormone. First, locally generated dopamine release signals are organized over more than four orders of magnitude (0.001 Hz- 10 Hz). Second, these dopamine events are finely-tuned within and between frequency domains as building blocks that recur over days to weeks. Third, an integration time window is detected across the median eminence, and consists of high-frequency dopamine discharges that are coordinated within the minutes range. Thus, a hierarchical combination of time-scaled neuroendocrine signals displays local-global integration to connect brain-pituitary rhythms and pace hormone secretion.

Significance Statement

The hypothalamo-pituitary axis controls a wide-range of homeostatic processes including growth, stress and reproduction. Despite this, the hypothalamic neuron firing patterns that lead to slowly-evolving pituitary hormone rhythms remain enigmatic. Here, we employed *in vivo* amperometric recordings in freely-behaving mice to investigate how tuberoinfundibular neurons release dopamine (DA) at the median eminence (ME) to control pituitary prolactin secretion. Using this approach, we show that DA release occurs as multiple locally-generated and time-scaled secretory events, which are integrated over a range of minutes across the ME. These results provide a broad physiological mechanism for the dialog that occurs between the brain and pituitary to dictate hormone rhythms over multiple timescales, from ultradian to seasonal.

MAIN TEXT

\body A remarkable function of the brain is its capability to integrate temporal information with complex physiological responses. This has been well established for behavioral responses such as non–rapid eye movement (NREM) sleep, where three neuronal oscillations with distinct frequency bands support information transfer (1). Yet the neuronal mechanisms that orchestrate the dialog between the brain and other basic functions like reproduction, lactation and growth remain largely unknown (2-5). They depend on the fine tuning of pituitary hormone pulses by small assemblies of hypothalamic neuroendocrine or parvocellular neurons, which release specific secretagogues at the median eminence (ME) (4, 6).

Here, we took advantage of the anatomical organisation of the ME to investigate how the tuberoinfundibular (TIDA) neuronal population (7, 8) releases dopamine (DA) to negatively regulate pituitary secretion of prolactin (PRL), a key reproductive hormone (2). To do so, miniaturized amperometric carbon fiber implants were used to detect DA release events (9) for days to weeks in freely-behaving mice. Using this approach, we uncovered a hierarchically-organized delivery of release events over four orders of magnitude (from <0.1 sec to several hours), which correlate with the dynamics of PRL in the bloodstream.

RESULTS

Frequency-coding of DA release events *in vivo*

To characterize the release dynamics of TIDA nerve terminals *in vivo*, we employed long-term constant voltage amperometry in awake mice using thin (30 µm tip diameter) carbon fibers implanted into the ME (Fig. 1A). Voltage was clamped at - 700 mV to allow detection of DA released from TIDA neurons. DA amperometry was performed continuously during several days, and the relationship with PRL secretion was assessed using tail blood micro-sampling for high-sensitivity mPRL ELISA developed in-house (10) (Fig. 1A). Single carbon fiber electrode recordings revealed robust DA currents (median 325 nA, IQR: 127 to 822 nA) due to oxidation of DA to dopamine-o-quinone (Fig. 1A), and these could be robustly detected over the long term (Fig.1B) (*n* = 7 virgin female mice). We then used DA as a relevant readout to explore the dynamics of TIDA neuron population function in freely-behaving animals. DA currents at the ME level discharged over different timescales (Fig. 1B, C) and more frequently during the night than day (Fig. 1D) (mean counts/h from ZT 0, in 6 hour blocks: 18.7, 27.2, 28.6, 30.4), implying that the strength of TIDA neuron excitability is likely modular around the day/night switch. DA release events were often grouped and interspaced by long-lasting (dozens of minutes to several hours) silent periods, suggesting nested relations between high and low frequency output patterns (Fig. 1B,C). No clear association between DA current density and estrus cycle stage was detected (Fig. 1C and Fig. S1).

Analysis of inter-event intervals (IEI) for DA release unveiled a wide range of time intervals, from less than 100 ms to a few hours, with two principal frequencies of 1.5 Hz and 12 Hz (Fig, 1E). Elevated release from TIDA neurons corresponded with periods of lowered PRL concentration (Fig. 1F). A delay of several minutes between decreasing PRL levels and the onset of high-frequency DA release events was also observed following exogenous PRL injection (Fig. 1G), and these occurred at similar frequencies (0.9 Hz and 17 Hz) (Fig. 1H) to those recorded during spontaneous activity (Fig. 1E). Notably, this response outlasted the decrease in PRL levels (Fig. S2), supporting a role for persistent PRL receptor signaling (2, 11, 12) or other mediators (13-15) in the generation of high-frequency DA release events.

Conversely, the arrest of high frequency DA release events was followed a few minutes later by an increase in PRL levels (Fig. 1F,I), resembling the previously described responses to administration of a

D2 receptor antagonist (10). Thus, the TIDA neuron population has the capability to generate bouts of DA release events at relatively high frequencies (Hz range), which are inversely correlated with PRL levels in the bloodstream of freely-moving mice. We were also able to record these episodic high-frequency DA events over a number of days during lactation (Fig. S3), although their amplitude and frequency were lower, most likely due to the reported loss of DA granular content at this time (9).

Long-range organization of DA release events at the local ME level

We next examined whether these sub-second DA release events possess a secondary/tertiary organization at the local level *i.e.* in the close vicinity of carbon fiber tips. Using cluster analysis to group DA currents on the basis of their shape, and bootstrapping to identify temporal series of events appearing with a higher-than-chance frequency during the recording period, a specific distribution could be revealed. In 6 of the 7 recorded mice, several repetitive patterns of DA release events were found, with stereotypical features remaining consistent between different animals recorded on different days (Fig. 2A, Fig. S4).

Further analyses demonstrated that these stereotyped patterns of DA release were not randomly-distributed, but rather appeared as chains of sequential events within the same group and/or between groups (Fig. 2 B-E). These recurrent motifs of DA release events were scaled from the millisecond (Fig. 2B-D) right up to the hour (Fig. 2E) range, and could even be detected over days (Fig. 2F-I). Thus, the mechanisms controlling TIDA neuron activities appear to be inherently robust.

Local-global integration of DA release events across the median eminence

A long-standing question regarding parvocellular neuron function is how nerve terminals discharge their neurohormones across the ME to sculpt pituitary output (2-4, 6). Given that TIDA nerve terminals abut over the whole ME (7, 8), dual-carbon fiber recordings were carried out 500 µm apart rostro-caudally, spanning the population (n = 3 animals). While distant DA events at high frequencies (≥1 Hz) were not synchronized (Fig. 3A), DA events were coordinated with IEI's in the minutes range during most of the recordings (Fig. 3B, C). This temporal coordination was not seen when each electrode was considered separately (Fig. 3D), suggesting that it is not simply due to hypothalamic PRL feedback, but rather effects on TIDA neuron interactions. Frequencies of 1.39 ± 0.12 Hz and 10.08 ± 2.6 Hz were both present during the dual electrode recordings of coordinated DA release events (n = 6) (Fig. 3E, F). Such spatial organization strengthens the view of a large-scale coordination within the TIDA neuron population, which may provide a means for transforming short-lived hypothalamic signals into long-lasting inputs for downstream endocrine targets.

DISCUSSION

Our results show how an ensemble of parvocellular TIDA neurons delivers its neuroendocrine products towards ME portal vessels in a freely-behaving mouse model. DA release events are repeated over weeks as network-driven rhythms that cover more than four orders of magnitude of frequency, from infra-slow (<0.001 Hz) to fast rhythms (1-10Hz). This organization occurs not only locally within, but also across the TIDA neuron assembly, as DA release events are scaled over the minute-range throughout the ME (Fig. 4).

Specifically, the use of miniaturized carbon fibers stereotaxically-implanted into the ME allowed us to detect and discriminate DA-related currents *in vivo*, which were far more complex, but also more organized than spike firing activities recorded in parvocellular neurons from either brain slices (9, 14-17) or anesthetized animals (18). Even though the small tip of the carbon fiber was likely able to detect DA release from only a few TIDA neurons, we observed a variety of rhythms. First, high frequency (about 1 and 10 Hz) events were prominent locally but not synchronized globally. As the site of recording is variable and these rhythms were observed in all animals, a large number of local

DA release processes presumably originate from TIDA neurons capable of secreting at high rates. The latter would be considered as “executive” in the top-down control of pituitary PRL rhythms by hypothalamic DA inputs, since they coincided with drops in pituitary PRL secretion. Second, slower rhythms of DA release (with time periods of minutes to hours) were detectable locally due to the ability of small carbon fibers to measure DA events over days to weeks with no noticeable deleterious effects. Strikingly, these were not distinguishable from high frequency DA events with which a hierarchal combination occurred regarding both the specific frequencies generated and how they organize in time as temporal motifs. Since the local-global integration of high frequency DA events occurred over frequencies of one or more minutes across the ME, slow rhythms may orchestrate the delivery of longer, but highly-ordered DA outputs from the TIDA neuron assembly towards the pituitary responder.

The current study performed in freely-behaving animals poses the question of how the TIDA neuronal network generates such a hierarchal organization of DA release events *in vivo*. While classical PRL feedback (2) is able to account for a proportion of the high frequency DA release events through direct stimulation of TIDA neuron electrical activity, it cannot explain slower rhythms including those organized over a minutes-range across the ME. This raises the possibility that both intra-network modes of information transfer (14, 19) and neuronal inputs (13-16), which were recently revealed in acute brain slice studies, may contribute to the coding of DA release at the ME level. Nonetheless, the present study suggests that the TIDA neuron network has the inherent capability to code DA release over time periods consistent with the pacing of PRL secretion.

Finally, it has recently been shown that local somatodentritic DA release from the TIDA population is able to influence close neuronal neighbours within the arcuate nucleus (19). As D1 and D2 receptors are expressed in the ME (20), this raises the possibility that DA release events at the ME, even those organized over slow rhythms, may also contribute to the regulation of other neurohormones, such as those underlying circhoral luteinizing- and growth-hormone pulses (20, 21).

The discovery of a multiple-time-scale integration of DA delivery at the neurohemal space provides a hitherto unknown element concerning how the brain dialogs with peripheral organs via a neuroendocrine connection. Such hierarchical organization of rhythms has been observed in other brain regions where multiple oscillations co-occur, with the slower oscillation generally driving local, faster oscillations (1). A similar multiple-time-scale neurohemal code may plausibly be shared by other assemblies of hypothalamic parvocellular neurons. Notably, the ME is capable of delivering hormone changes over a wide-range of timescales, from ultradian to seasonal (22, 23). This neurohemal structure may thus provide a model system for investigating how parvocellular outputs are translated into slowly-evolving endocrine outcomes such as reproduction, growth, metabolism and stress.

MATERIALS AND METHODS

Detailed methods are provided in SI Materials and Methods. Briefly, carbon fiber microelectrodes were fabricated using a single 30µm thread of carbon fiber, coated in Nafion and connected to a gold-plated pin. C57/BL6 female mice were stereotaxically implanted with carbon fiber microelectrodes at the level of the median eminence (stereotaxic coordinates (relative to Bregma) -1.3 mm rostro-caudal; 0 mm medio-lateral; 6.1 mm ventral). After recovery, mice were transferred to recording cages, connected to an electrical swivel to allow for free movement, and carbon fibers were held at 700 mV throughout the recording to detect secretion of DA. Repeated tail blood microsampling was performed to measure blood PRL levels, using a home-made ELISA. All statistical analysis was performed with R software.

ACKNOWLEDGEMENTS

P.M. was supported by grants from the Agence Nationale de la Recherche (ANR-06-BLAN-0322, ANR 12 BSV1 0032), Fondation pour la Recherche Médicale (DEQ20150331732), France-Bioimaging (ANR-10-INBS-04-03), Institut National de la Santé et de la Recherche Médicale, Centre National de la Recherche Scientifique, Université de Montpellier, Biocampus-Montpellier, IPAM-BCM, Région Languedoc Roussillon, and the National Biophotonics and Imaging Platform (Ireland). D.J.H. was supported by Diabetes UK R.D. Lawrence (12/0004431), EFSD/Novo Nordisk Rising Star and Birmingham Fellowships, a Wellcome Trust Institutional Support Award, a COMPARE primer grant, an MRC Project Grant (MR/N00275X/1), and an ERC-StG (OptoBETA; 715884). We thank Evelyne Galibert for assistance with animal breeding and maintenance.

CONTRIBUTIONS

N.R. designed and performed experiments, analyzed the data, and wrote the manuscript. A.G. performed experiments. D.J.H. analyzed the data and wrote the manuscript. A.O.M. and P.M. supervised the project, and contributed to experimental design, data analysis and writing of the manuscript.

COMPETING FINANCIAL INTEREST

The authors declare no competing financial interests.

REFERENCES

1. Buzsaki G, Logothetis N, & Singer W (2013) Scaling brain size, keeping timing: evolutionary preservation of brain rhythms. *Neuron* 80(3):751-764.
2. Grattan DR (2015) 60 years of neuroendocrinology: The hypothalamo-prolactin axis. *The Journal of endocrinology* 226(2):T101-122.
3. Herbison AE (2016) Control of puberty onset and fertility by gonadotropin-releasing hormone neurons. *Nature reviews. Endocrinology* 12(8):452-466.
4. Le Tissier P*, et al.* (2016) An updated view of hypothalamic-vascular-pituitary unit function and plasticity. *Nature reviews. Endocrinology* doi:10.1038/nrendo.2016.193
5. Le Tissier PR*, et al.* (2012) Anterior pituitary cell networks. *Frontiers in neuroendocrinology* 33(3):252-266.
6. Harris GW (1951) Neural control of the pituitary gland. II. The adenohypophysis, with special reference to the secretion of A.C.T.H. *British medical journal* 2(4732):627-634.
7. Ajika K & Hokfelt T (1973) Ultrastructural identification of catecholamine neurones in the hypothalamic periventricular-arcuate nucleus-median eminence complex with special reference to quantitative aspects. *Brain research* 57(1):97-117.
8. Ibata Y & Watanabe K (1977) A morphological survey of the median eminence: fluorescence histochemistry, electron microscopy and immunohistochemistry. *Archivum histologicum Japonicum* 40 Suppl:303-315.
9. Romano N*, et al.* (2013) Plasticity of hypothalamic dopamine neurons during lactation results in dissociation of electrical activity and release. *The Journal of neuroscience* 33(10):4424-4433.
10. Guillou A*, et al.* (2015) Assessment of lactotroph axis functionality in mice: longitudinal monitoring of PRL secretion by ultrasensitive-ELISA. *Endocrinology* 156(5):1924-1930.
11. Bernard V, Young J, Chanson P, & Binart N (2015) New insights in prolactin: pathological implications. *Nature reviews. Endocrinology* 11(5):265-275.

12. Goffin V & Touraine P (2015) The prolactin receptor as a therapeutic target in human diseases: browsing new potential indications. *Expert opinion on therapeutic targets* 19(9):1229-1244.
13. Briffaud V, Williams P, Courty J, & Broberger C (2015) Excitation of tuberoinfundibular dopamine neurons by oxytocin: crosstalk in the control of lactation. *The Journal of neuroscience* 35(10):4229-4237.
14. Lyons DJ, Horjales-Araujo E, & Broberger C (2010) Synchronized network oscillations in rat tuberoinfundibular dopamine neurons: switch to tonic discharge by thyrotropin-releasing hormone. *Neuron* 65(2):217-229.
15. Zhang X & van den Pol AN (2015) Dopamine/tyrosine hydroxylase neurons of the hypothalamic arcuate nucleus release GABA, communicate with dopaminergic and other arcuate neurons, and respond to dynorphin, met-enkephalin, and oxytocin. *The Journal of neuroscience* 35(45):14966-14982.
16. Lyons DJ, Ammari R, Hellysaz A, & Broberger C (2016) Serotonin and antidepressant SSRIs inhibit rat neuroendocrine dopamine neurons: parallel actions in the lactotrophic axis. *The Journal of neuroscience* 36(28):7392-7406.
17. Lyons DJ, Hellysaz A, & Broberger C (2012) Prolactin regulates tuberoinfundibular dopamine neuron discharge pattern: novel feedback control mechanisms in the lactotrophic axis. *The Journal of neuroscience* 32(23):8074-8083.
18. Constantin S, Iremonger KJ, & Herbison AE (2013) In vivo recordings of GnRH neuron firing reveal heterogeneity and dependence upon GABAA receptor signaling. *The Journal of neuroscience* 33(22):9394-9401.
19. Stagkourakis S, Kim H, Lyons DJ, & Broberger C (2016) Dopamine autoreceptor regulation of a hypothalamic dopaminergic network. *Cell reports* 15:735-747.
20. Romero-Fernandez W*, et al.* (2014) Dopamine D1 and D2 receptor immunoreactivities in the arcuate-median eminence complex and their link to the tubero-infundibular dopamine neurons. *European journal of histochemistry* 58(3):2400.
21. Fuxe K*, et al.* (1986) Medianosomes as integrative units in the external layer of the median eminence. Studies on grf/catecholamine and somatostatin/catecholamine interactions in the hypothalamus of the male rat. *Neurochemistry international* 9(1):155-170.
22. Lincoln GA, Clarke IJ, Hut RA, & Hazlerigg DG (2006) Characterizing a mammalian circannual pacemaker. *Science* 314(5807):1941-1944.
23. Walker JJ*, et al.* (2012) The origin of glucocorticoid hormone oscillations. *PLoS biology* 10(6):e1001341.
24. Hulthe P, Hulthe B, Johannessen K, & Engel J (1987) Decreased ascorbate sensitivity with nafion-coated carbon fibre electrodes in combination with copper(II) ions for the electrochemical determination of electroactive substances in vivo. *Anal. Chim. Acta* 198**:**197-206.
25. Perkel DH, Gerstein GL, & Moore GP (1967) Neuronal spike trains and stochastic point processes. II. Simultaneous spike trains. *Biophysical journal* 7:419-440.

FIGURE LEGENDS

Fig. 1. *In vivo* monitoring of DA release events at the median eminence level. (*A*) Electrodes were implanted at the median eminence (ME) of mice and dopamine (DA) was detected using constant voltage amperometry. Serial blood micro-sampling was performed from the tail vein. (*B*) Representative 24 hour recording of DA release (*top, shaded area is lights-out*), with zoom of a 10-minute sequence (*bottom*). (*C*) Representative 11 day recording from a female mouse. Each vertical line corresponds to a single secretion event. The stage of the estrous cycle is indicated on the left for each day (M, metestrous; D, diestrous; P, proestrous, E, estrous). (D) Mean distribution of DA release events during the day (*n* = 80 days from 7 female mice). (*E*) Histogram of inter-event intervals (IEIs): two prominent frequencies are apparent at 1.5 and 12 Hz (*n* = 80 days, from 7 female mice). (*F*) Relation between DA and PRL. Average normalized PRL levels occurring around a DA event (*n* = 501 DA events, from six 1 hour long sessions) (black, mean; blue, SEM). *(G)* DA secretory response to a i.p. injection of 1µg ovine PRL (PRL injected at time 0) (from 5 animals, 7 injections). *(H)* Distribution of the IEIs of DA events induced by i.p. injection of PRL. *(I)* Example of simultaneous recording of PRL levels (red) and DA release events (black). In all cases, bar graphs show the mean ± SEM.

Fig. 2. Temporal patterning of DA release events. (*A)* Distribution of IEIs for each class of event obtained after clustering all events from one recording by shape (*n* = 13541). Insets show average event shape in each group; the proportion of each class is shown near each graph. (*B-E*) Example of temporal patterns on DA release. Each dot represents a single DA release event, colored depending on the subgroup (as in figure 2A). Each line shows one repetition of the sequence during the recording; five examples of repetition are shown for each pattern. (*F-I*) Frequency of the four temporal patterns during 8 days of recording.

Fig. 3. Spatial patterning of DA release events. (*A*) Representative double recording of DA secretion at distant sites in the ME (500 µm rostro-caudal), showing de-synchronization of release events at the minute timescale. (*B*) Distribution of events from a double recording. *Top:* "rug plot" of DA release events, where each vertical line represents one event detected by one of the two electrodes. *Bottom:* density plot of the DA events, showing coincidence over a long time scale. (*C*) Cross-distribution of IEI between the two electrodes, showing reciprocal delays during a ~7 minute time lag. *(D)* Auto-correlation of the signals on each of the single electrodes only shows the expected peak at lag 0, suggesting that the coordination is not dependent on pituitary feedback. *(E-F)* Distribution of IEIs from the signals detected by the two electrodes during a period in which DA release was only detected by one electrode *(E) (light purple)* or during a period of coordination between both electrodes *(F) (light purple and green; dark purple shows overlap of IEIs between both electrodes).*

Fig. 4. Schematic of the brain-pituitary dialog proposed to underlie hypothalamic dopaminergic control of pituitary prolactin secretion. Illustrated are three sub-sets of hypothalamic TIDA neurons (colored in green, brown and magenta), which each locally release dopamine (DA) at the median eminence level (where the first loop of portal capillaries reside). Local DA release events are organized in the frequency domain (0.001 Hz-10 Hz) and recur as sequences. Local-global integration across the median eminence coordinates high frequency DA release events within the minutes range. This allows the build-up of DA in the portal blood required to efficiently inhibit pituitary prolactin secretion.

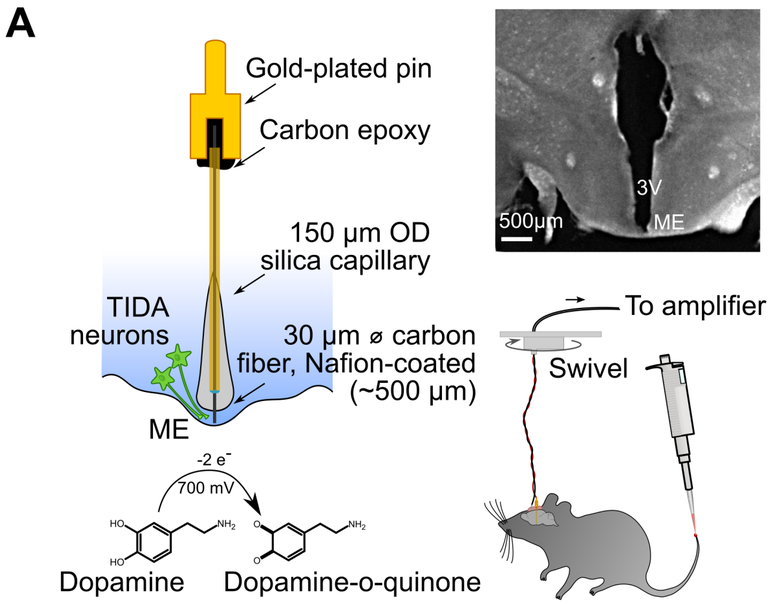
A
Gold-plated pin
Carbon epoxy
150 µm OD
silica capillary
TIDA
neurons
30 µm ⌀ carbon
fiber, Nafion-coated
(~500 µm)
ME
-2 e⁻
700 mV
Dopamine
Dopamine-o-quinone
3V
ME
500µm
To amplifier
Swivel

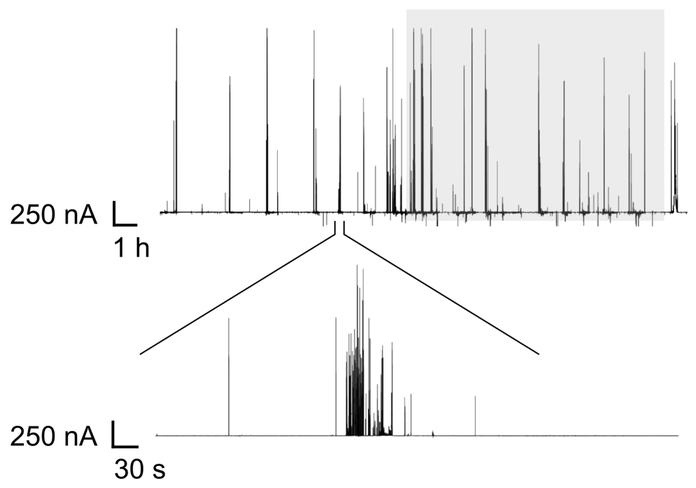
B
250 nA
1 h
250 nA
30 s

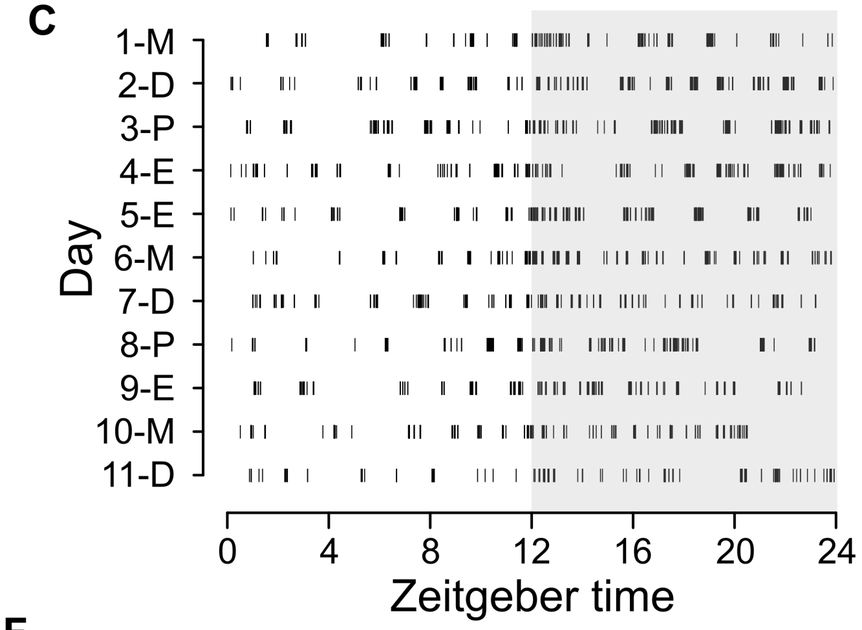
C
1-M
2-D
3-P
4-E
5-E
6-M
7-D
8-P
9-E
10-M
11-D
Day
0
4
8
12
16
20
24
Zeitgeber time

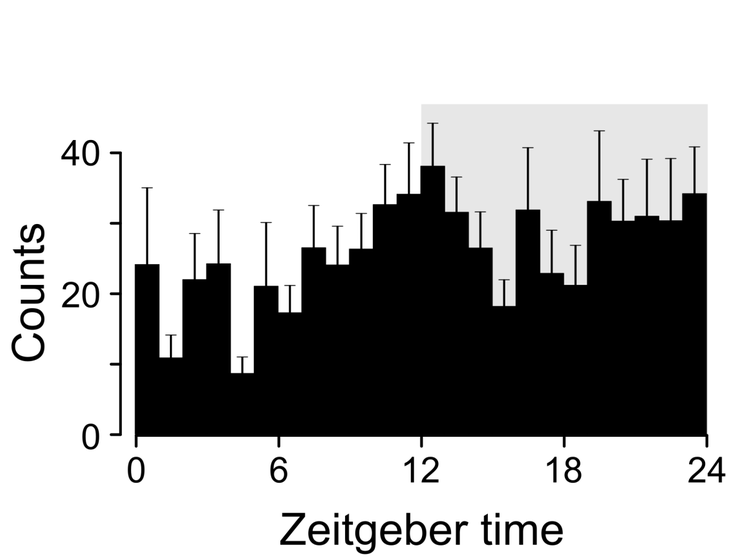
D
Counts
0
20
40
0
6
12
18
24
Zeitgeber time

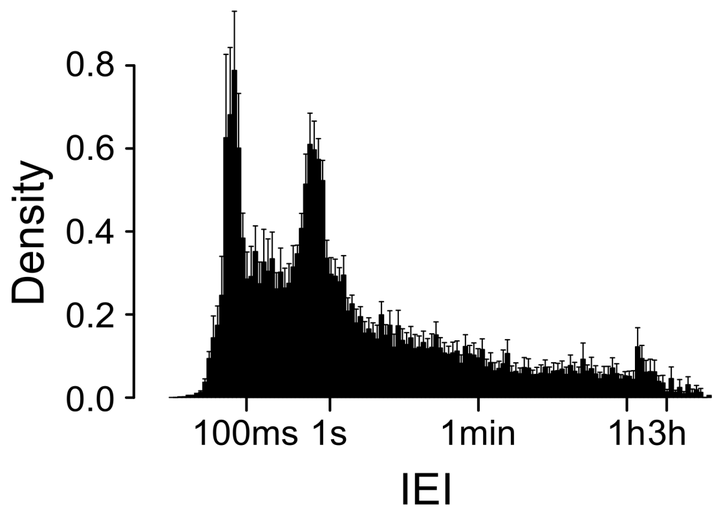
E
Density
0.0
0.2
0.4
0.6
0.8
100ms
1s
1min
1h
3h
IEI

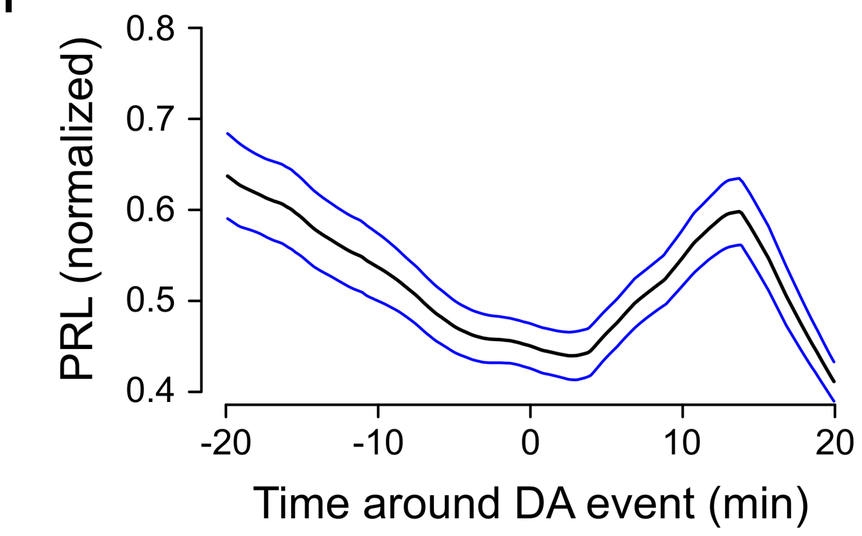
F
PRL (normalized)
0.4
0.5
0.6
0.7
0.8
-20
-10
0
10
20
Time around DA event (min)

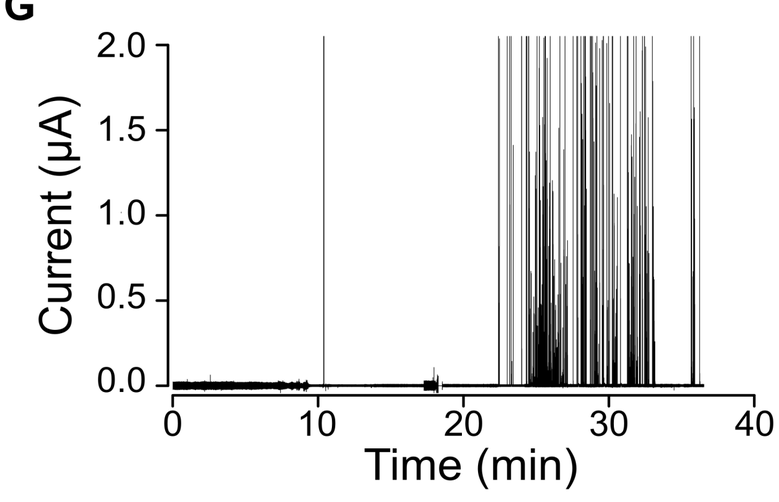
G
Current (µA)
0.0
0.5
1.0
1.5
2.0
0
10
20
30
40
Time (min)

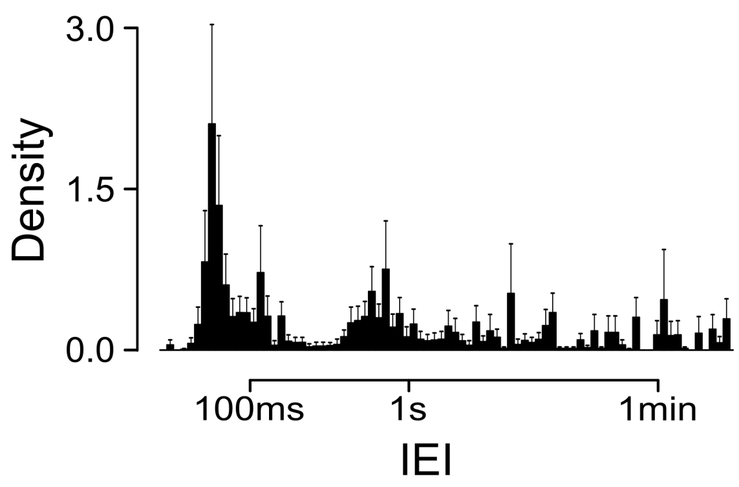
H
Density
0.0
1.5
3.0
100ms
1s
1min
IEI

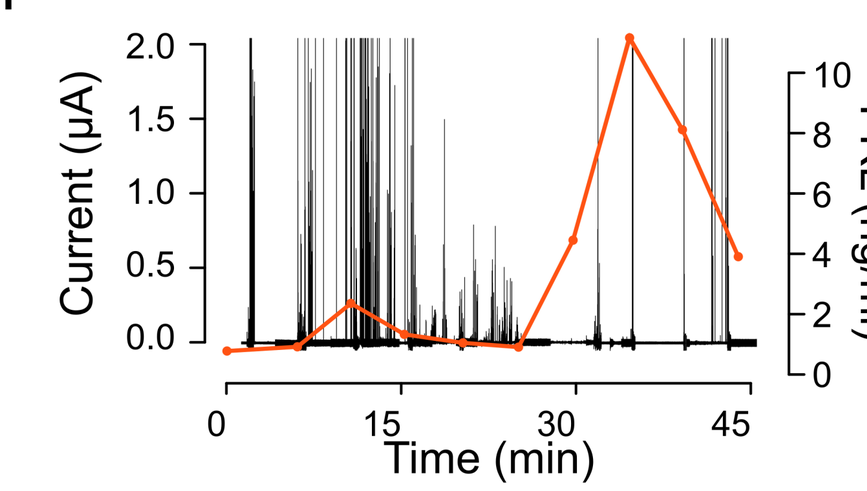
I
Current (µA)
0.0
0.5
1.0
1.5
2.0
PRL (ng/ml)
0
2
4
6
8
10
0
15
30
45
Time (min)

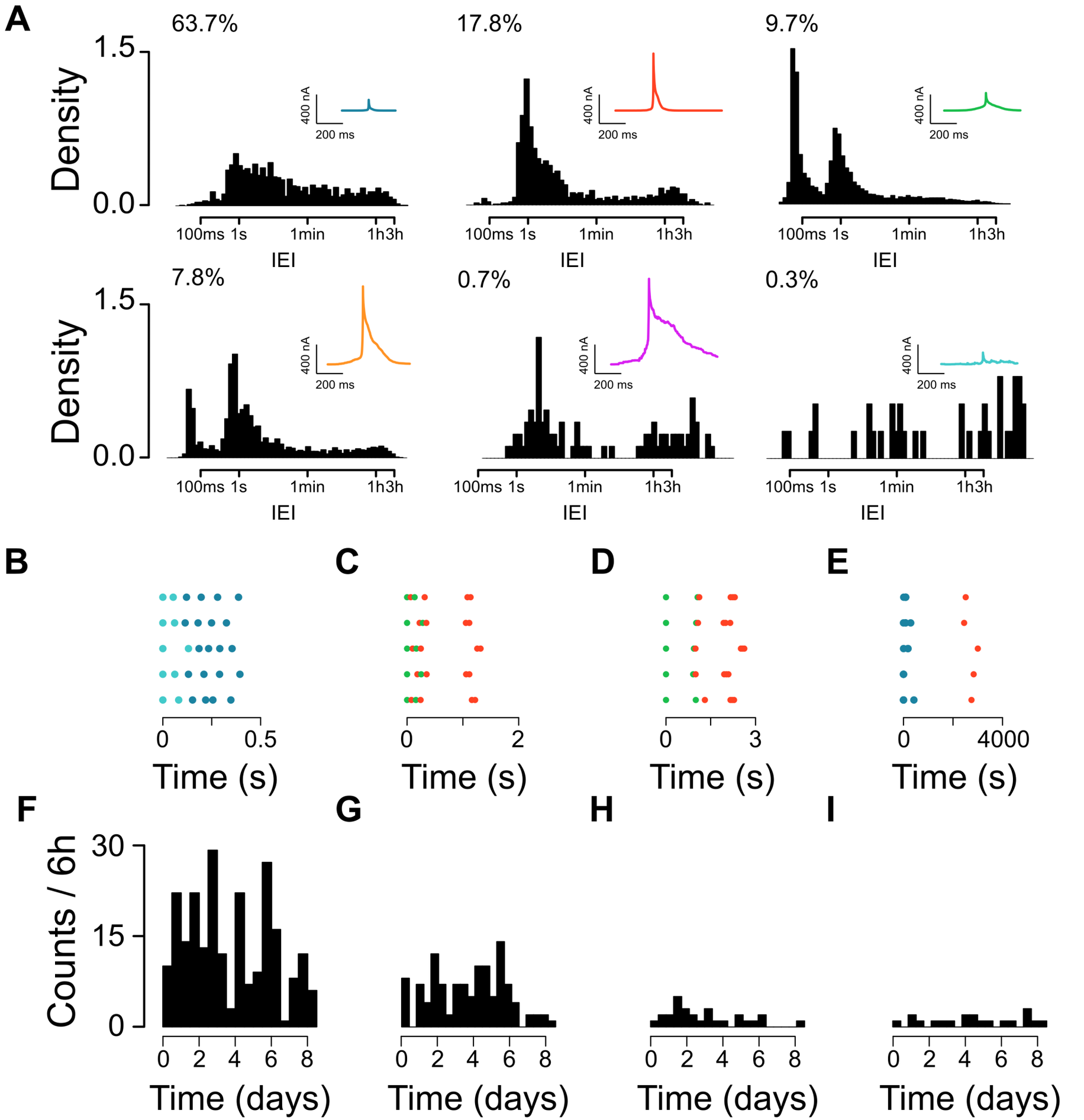
A
63.7%
17.8%
9.7%
7.8%
0.7%
0.3%
Density
1.5
0.0
400 nA
200 ms
100ms 1s 1min 1h3h
IEI
B
C
D
E
0 0.5
0 2
0 3
0 4000
Time (s)
F
G
H
I
Counts / 6h
30
15
0
0 2 4 6 8
Time (days)

A

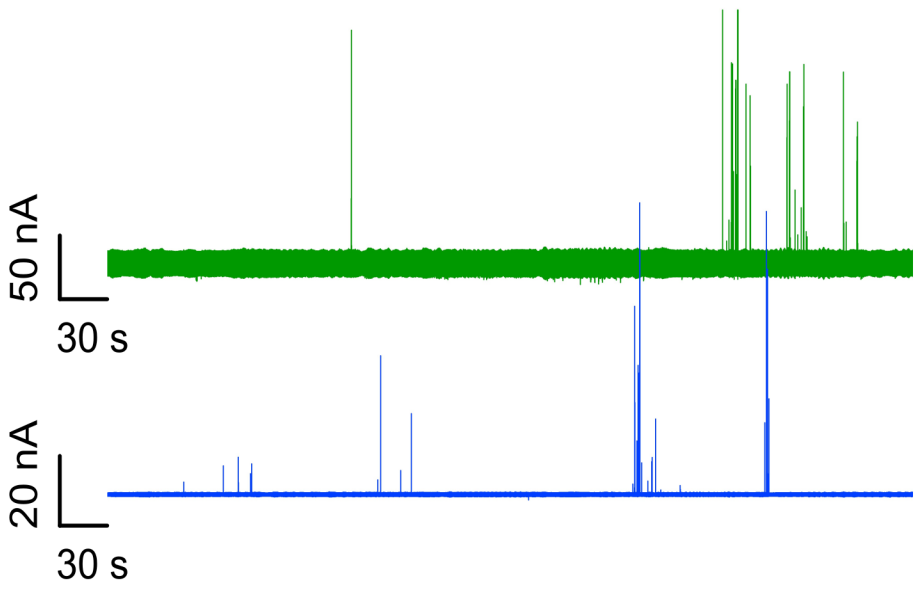
50 nA
30 s
20 nA
30 s

B

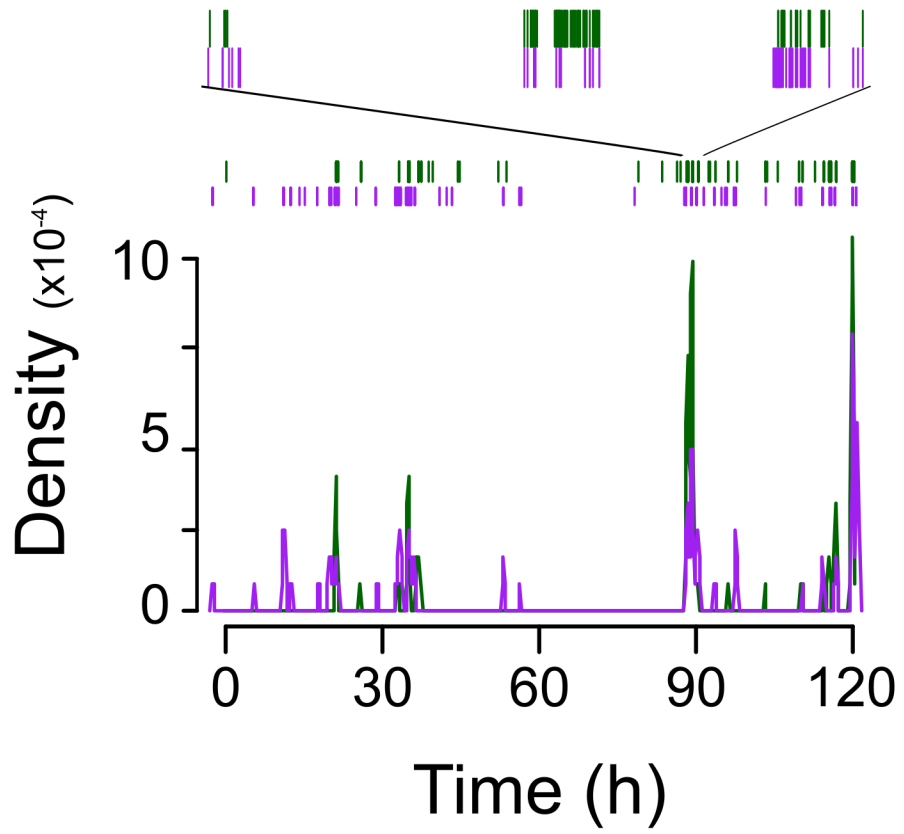
Density (x10-4)
10
5
0
0
30
60
90
120
Time (h)

C

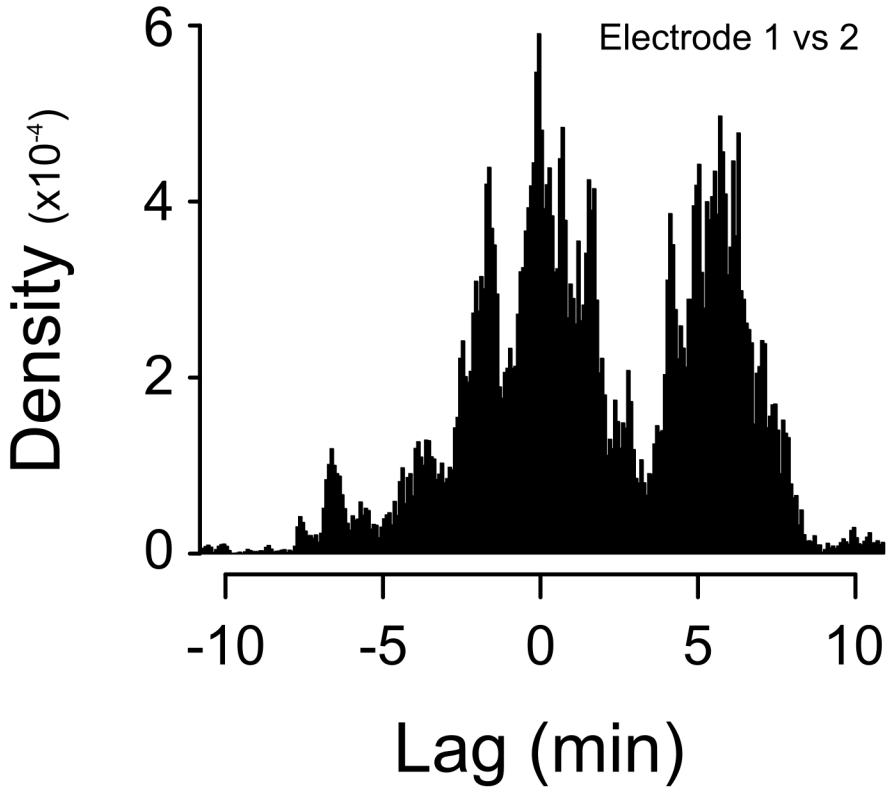
Electrode 1 vs 2
Density (x10-4)
6
4
2
0
-10
-5
0
5
10
Lag (min)

D

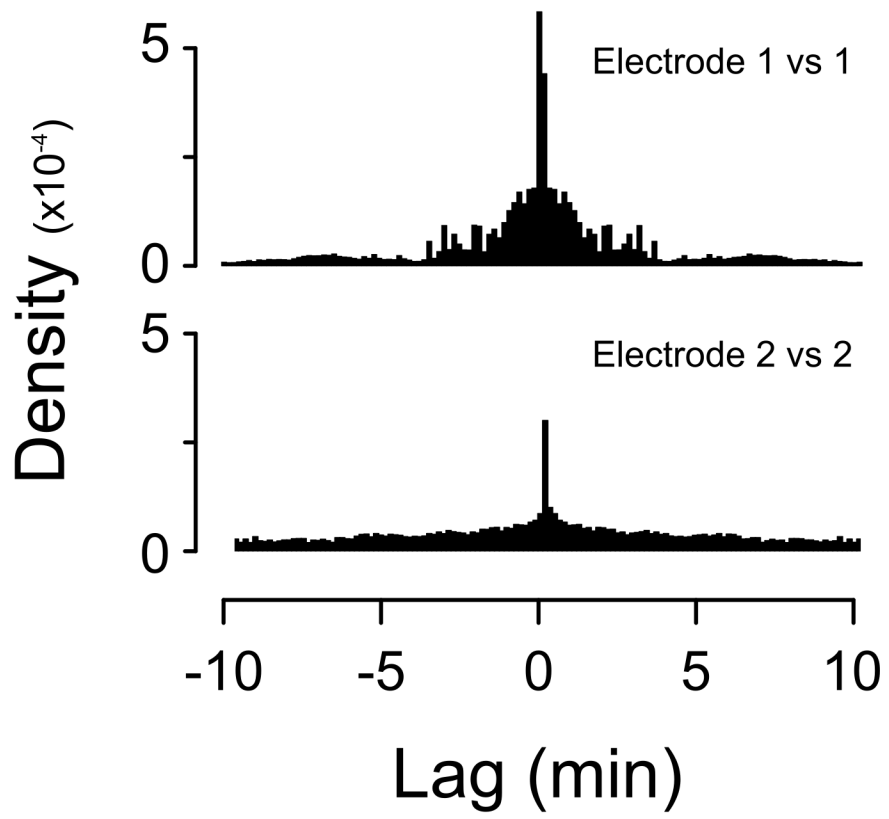
Electrode 1 vs 1
Electrode 2 vs 2
Density (x10-4)
5
0
5
0
-10
-5
0
5
10
Lag (min)

E

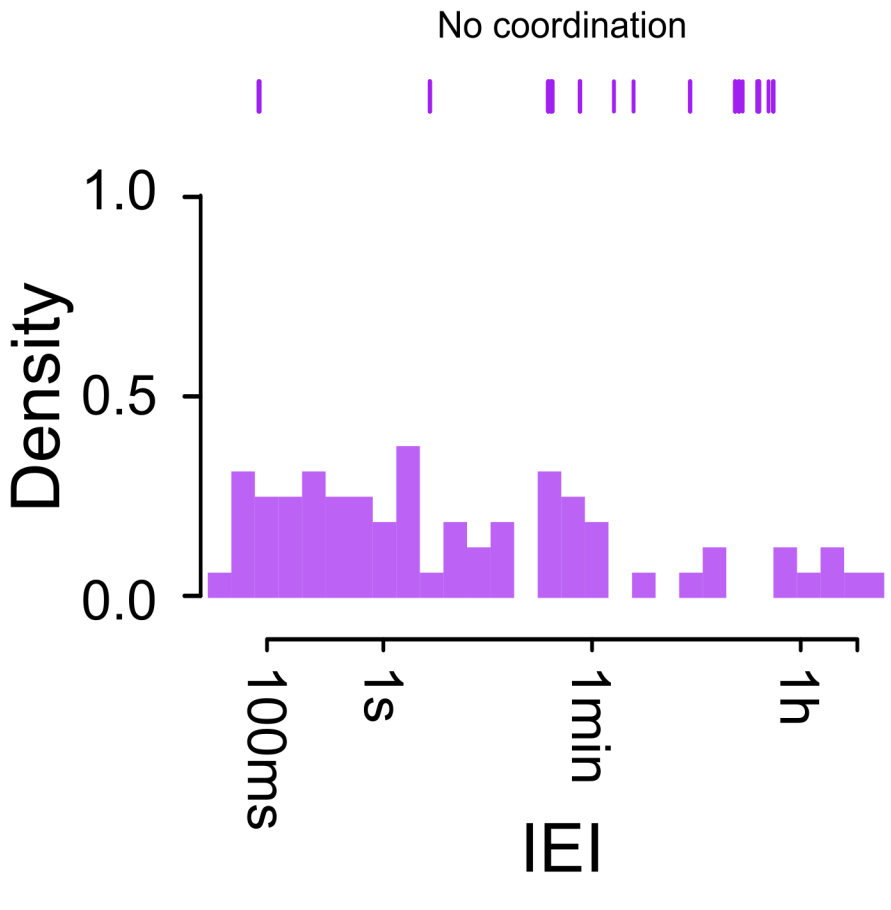
No coordination
Density
1.0
0.5
0.0
100ms
1s
1min
1h
IEI

F

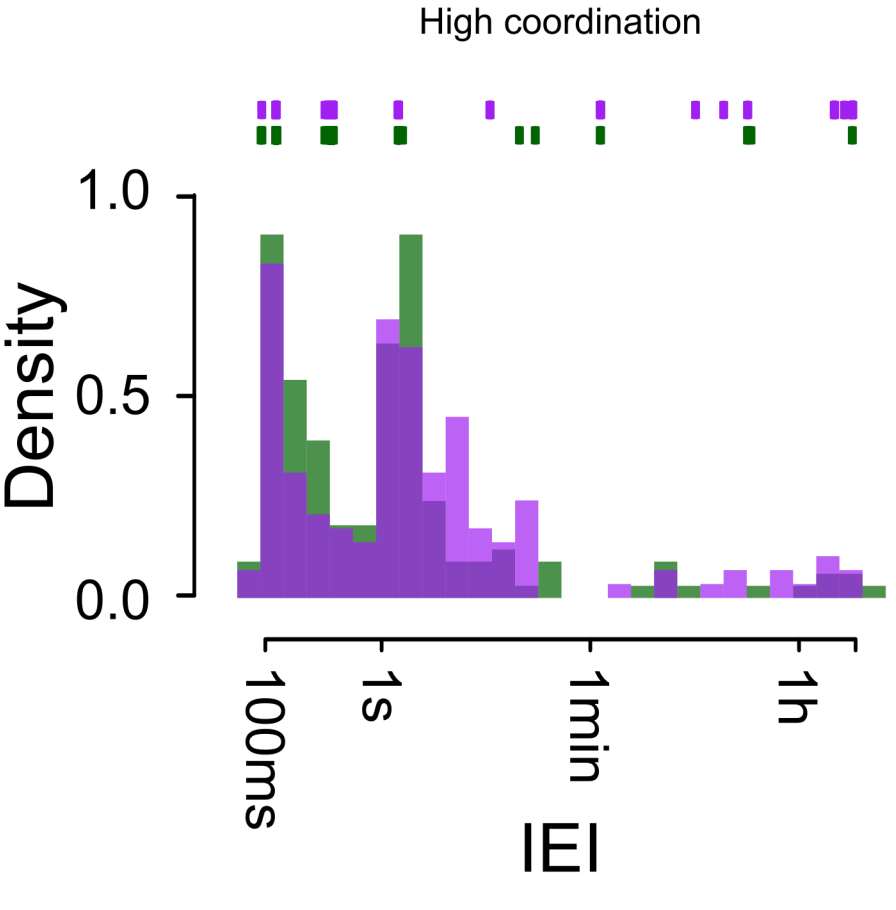
High coordination
Density
1.0
0.5
0.0
100ms
1s
1min
1h
IEI

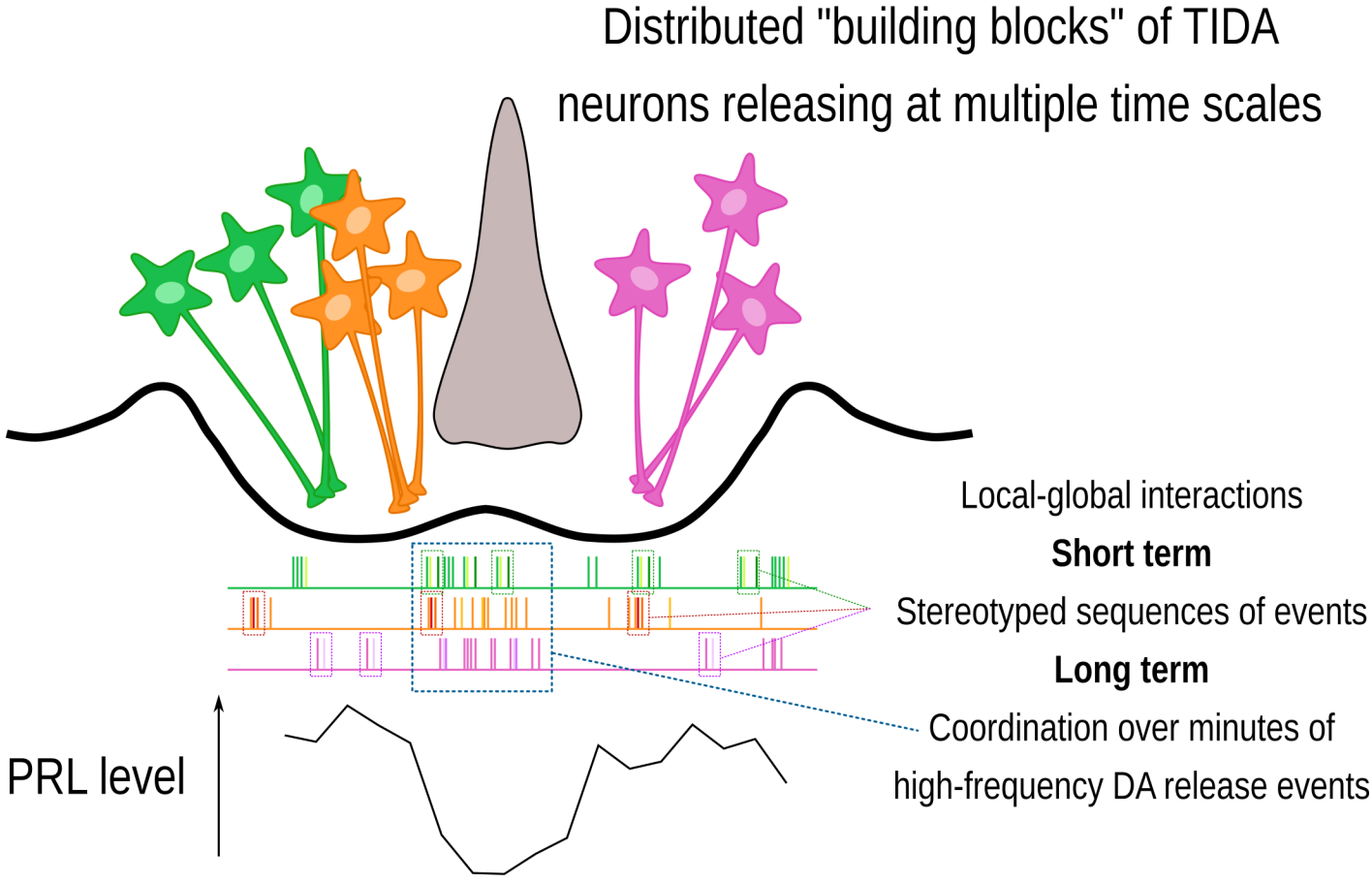
Distributed "building blocks" of TIDA
neurons releasing at multiple time scales
Local-global interactions
Short term
Stereotyped sequences of events
Long term
Coordination over minutes of
high-frequency DA release events
PRL level